© 2018. Published by The Company of Biologists Ltd | Journal of Experimental Biology (2018) 221, jeb167742. doi:10.1242/jeb.167742

RESEARCH ARTICLE

Myosin phosphorylation potentiates steady-state work output without altering contractile economy of mouse fast skeletal muscles

William Gittings, Jordan Bunda and Rene Vandenboom*

ABSTRACT

Skeletal myosin light chain kinase (skMLCK)-catalyzed phosphorylation of the myosin regulatory light chain (RLC) increases (i.e. potentiates) mechanical work output of fast skeletal muscle. The influence of this event on contractile economy (i.e. energy cost/work performed) remains controversial, however. Our purpose was to quantify contractile economy of potentiated extensor digitorum longus (EDL) muscles from mouse skeletal muscles with (wild-type, WT) and without (skMLCK ablated, skMLCK$^{-/-}$) the ability to phosphorylate the RLC. Contractile economy was calculated as the ratio of total work performed to high-energy phosphate consumption (HEPC) during a period of repeated isovelocity contractions that followed a potentiating stimulus (PS). Consistent with genotype, the PS increased RLC phosphorylation measured during, before and after isovelocity contractions in WT but not in skMLCK$^{-/-}$ muscles (i.e. 0.65 and 0.05 mol phosphate mol^{-1} RLC, respectively). In addition, although the PS enhanced work during repeated isovelocity contractions in both genotypes, the increase was significantly greater in WT than in skMLCK$^{-/-}$ muscles (1.51±0.03 versus 1.10±0.05, respectively; all data P<0.05, n=8). Interestingly, the HEPC determined during repeated isovelocity contractions was statistically similar between genotypes at 19.03±3.37 and 16.02±3.41 μmol P; respectively (P<0.27). As a result, despite performing significantly more work, the contractile economy calculated for WT muscles was similar to that calculated for skMLCK$^{-/-}$ muscles (i.e. 5.74±0.67 and 4.61±0.71 J kg^{-1} μmol^{-1} P, respectively (P<0.27). In conclusion, our results support the notion that myosin RLC phosphorylation enhances dynamic contractile function of mouse fast skeletal muscle but does so without decreasing contractile economy.

KEY WORDS: Potentiation, Regulatory light chain, Myosin light chain kinase knockout, Economy, Energetics

INTRODUCTION

Repetitive or sustained activation of fast skeletal muscles invariably leads to progressive reductions in contractile function known as fatigue. The reductions in force, work or power observed during fatigue may be due to reductions in either the maximal calcium (Ca^{2+})-activated force or the Ca^{2+} sensitivity of force development, or both (Westerblad et al., 2010). These alterations to excitation–contraction coupling may compromise mechanical function but help to preserve ATP homeostasis during prolonged muscle activity (Macintosh et al., 2012; Myburgh, 2004). Thus, because fatigue is such a prominent characteristic of the fast fiber phenotype across the animal kingdom, there is considerable interest in peripheral factors that might preserve contractile function during sustained muscular activity.

Rodent fast skeletal fibers contain the enzymatic apparatus for rapidly phosphorylating the myosin regulatory light chain (RLC), a mechanism thought to provide a 'molecular memory' of contractile history (Stull et al., 2011). Indeed, in permeabilized skeletal muscle fibers, RLC phosphorylation has been demonstrated to increase the Ca^{2+} sensitivity and/or the maximal Ca^{2+}-activated force of the contractile proteins (Godt and Nosek, 1989; Persechini et al., 1985). These outcomes may account for why stimulation-induced elevations in RLC phosphorylation are so strongly associated with isometric twitch force potentiation in a variety of rodent skeletal muscle models (reviewed by Vandenboom et al., 2013). This modulation of contractile protein function by RLC phosphorylation may extend into fatigue as twitch potentiation has been reported to coexist with reductions in tetanic force (Gordon et al., 1990; Rankin et al., 1988; Rassier and Macintosh, 2000; Vandenboom and Houston, 1996). Given the metabolic consequences of fatigue, the ability of RLC phosphorylation to modulate contractile performance may hinge critically upon how this molecular mechanism influences muscle energetics, however. In this regard, early studies suggested that RLC phosphorylation decreased the energy cost for prolonged isometric tetani by reducing actomyosin turnover rate in mouse extensor digitorum longus (EDL) muscles (23°C) (Crow and Kushmerick, 1982a,b). Subsequent work using the same muscle model reported that no consistent relationships were evident between RLC phosphorylation and rate of ATP consumption and actomyosin cycling rate (Barsotti and Butler, 1984; Butler et al., 1983). Although the discrepancy in these papers may be due to the confounding influence of fatigue on actomyosin turnover rate, the influence of RLC phosphorylation on energetics of mouse fast muscle has remained an open question for approximately three decades.

In an attempt to resolve this issue, Abbate et al. (2001) measured high-energy phosphate consumption (HEPC) of unpotentiated and potentiated isovelocity contractions of rat gastrocnemius skeletal muscles *in situ* (35°C). Their results showed that a brief period of repetitive high-frequency stimulation increased RLC phosphorylation and concentric work compared with unpotentiated contractions. In addition, their chemical data showed that HEPC turnover, and thus the energetic cost, of potentiated contractions was higher than that in unpotentiated contractions. Importantly, potentiation increased HEPC turnover more than it increased work, thus reducing muscle economy. This effect was attributed to an increased energy cost of activation and/or

Centre for Bone and Muscle Health, Faculty of Applied Health Sciences, Brock University, St Catharines, ON L2S 3A1, Canada.

*Author for correspondence (rvandenboom@brocku.ca)

J.B., 0000-0001-9213-8709; R.V., 0000-0002-6838-6419

Received 4 August 2017; Accepted 28 October 2017

Journal of Experimental Biology (2018) 221, jeb167742. doi:10.1242/jeb.167742

List of abbreviations

Cr	creatine
$-dP/dt$	rate of force relaxation
$+dP/dt$	rate of force development
EDL	extensor digitorum longus
HEPC	high-energy phosphate consumption
L_o	optimal length (for peak muscle twitch force)
PCr	phosphocreatine
PCSA	physiological cross-sectional area
P_o	peak tetanic force
PS	potentiating stimulus
P_t	peak twitch force
RLC	regulatory light chain
skMLCK$^{-/-}$	myosin light chain kinase knockout (skeletal muscle isoform)
V_{max}	maximal shortening velocity

actomyosin ATPase associated with potentiation, and not to any increase in the energy cost for RLC phosphorylation observed between the two conditions (Abbate et al., 2001). An implication of these experiments is that, because economy is reduced, RLC phosphorylation-mediated potentiation may not represent a sustainable outcome for fast twitch skeletal muscle *in vivo* (Brown and Loeb, 1998).

A limitation of all previous work examining muscle economy is the concomitant increase in RLC phosphorylation with the onset of contractile activity, making it difficult to parse out the separate energetic requirements of these biochemical and mechanical events. The purpose of this work was to study the contractile economy of potentiated fast skeletal muscle during an intermittent period of steady concentric work output in the presence and absence of RLC phosphorylation. To this end, we quantified muscle economy (i.e. the work to HEPC ratio) during repeated isovelocity concentric contractions in potentiated EDL muscles from wild-type (WT) and myosin light chain kinase-devoid (skMLCK$^{-/-}$) mice. Our experimental design allowed us to assiduously compare the specific effect of RLC phosphorylation-mediated potentiation on total work and HEPC turnover, and thus economy, of working muscles. We hypothesized that WT muscles with RLC phosphorylation would perform significantly more work but would demonstrate disproportionate increases in HEPC turnover, and thus a reduced economy, compared with skMLCK$^{-/-}$ muscles without RLC phosphorylation.

MATERIALS AND METHODS

Study design

All animal handling procedures and techniques received prior approval from the Brock University Animal Care Committee. Adult male wild-type (WT; *Mus musculus* Linnaeus 1758, C57BL/6) mice (≥10 weeks) were sourced from Charles River Laboratories (St Constant, QC, Canada) and housed at Brock University. Age- and sex-matched (±2 months) sexually mature skMLCK$^{-/-}$ mice (*Mus musculus*, C57BL/6 background) from our breeding colony were entered into the study as needed. Body masses of mice used in this study were similar between genotypes (21.34±0.70 and 22.78±0.22 g for skMLCK$^{-/-}$ and WT mice, respectively). The characterization and development of the skMLCK$^{-/-}$ animals has been explained previously (Gittings et al., 2011, 2015, 2016; Zhi et al., 2005). No fiber-type differences between WT and skMLCK$^{-/-}$ mice have been detected (Gittings et al., 2011). For a recent discussion of issues related to genetic drift and our use of skMLCK$^{-/-}$ mice, see Bowslaugh et al. (2016). Identical experiments were conducted on the two genotypes to investigate the contractile economy of skeletal muscles with and without the capacity (skMLCK expression) to phosphorylate the RLC. Economy was calculated as the ratio of the total work done during a series of concentric contractions to HEPC as measured using fluorometric assays. On the day of an experiment, mice were anesthetized with an intraperitoneal injection of sodium pentobarbitol (60 mg kg^{-1} body mass). EDL muscles were surgically removed from both hindlimbs and immediately incubated at resting length in an oxygenated bath containing cooled Tyrode's solution (~5–10°C) until needed (Lännergren et al., 2000). Muscles were suspended vertically using non-compliant 4-0 silk suture in the 1200A intact muscle apparatus (Aurora Scientific Inc., Aurora, ON, Canada). The distal suture was clamped directly to the electrode assembly and the proximal suture was secured to the servomotor arm via a short stainless steel wire. Contractile experiments were conducted at 25°C with the muscle immersed in continuously gassed (95% O_2, 5% CO_2) Tyrode's solution (Lännergren et al., 2000).

Contractile experiments

Each experiment commenced with an incubation period of 30 min to allow the muscle to equilibrate: during this stage the stability of muscle twitch force was tracked using a single stimulation every 3 min (Model 701B, Aurora Scientific Inc., Aurora, ON, Canada). Stimulation intensity was set to ~1.25 times the voltage required for maximal twitch force to ensure that all fibers in the preparation were activated (≥60 V). Optimal length (L_o) was determined using the micrometer attached to the bath assembly and stimulating the muscle at small length increments (1–2% L_o) to find maximal twitch force. The experimental timeline and details of the isovelocity shortening ramps used are shown in Fig. 1. To measure concentric force and power, muscles were stimulated at 75 Hz for 50 ms during constant velocity shortening from 1.05 to 0.9 L_o. The rate of ramp shortening was equivalent to 40% of maximal shortening velocity as determined previously in our lab using the slack test (Gittings et al., 2011; see also Edman, 1979, for the original development of the technique). Stimulation was timed such that force was developed 2 ms after the start of shortening and force relaxation occurred just prior to the completion of the ramp. Identical passive ramps were conducted without stimulation to estimate the non-contractile force component and subtract it from the total force trace to yield an active force record, as previously described (Gittings et al., 2012, 2015, 2016). Concentric force potentiation is positively associated with shortening speed (Gittings et al., 2012; Brown and Loeb, 1999) and thus the relatively fast shortening ramps used in this study (0.40 V_{max}) were chosen to maximize this relationship.

Potentiating stimulus

Muscles of both genotypes were stimulated with four brief (400 ms) but high-frequency volleys (100 Hz) within a 10 s window, with muscle length held at 0.90 L_o, in order to potentiate the force and work of the concentric stimulation to follow. This potentiating stimulus (PS) has been shown to produce large elevations in RLC phosphorylation levels in EDL muscles with little or no fatigue (Gittings et al., 2011, 2012, 2015, 2016; Caterini et al., 2011; Xeni et al., 2011). Baseline measures of concentric force and power were collected using a single control stimulus that was applied prior to the PS. Following the PS, the isovelocity stimulation protocol was repeated 20 times at the rate of 1 stimulus per second.

Journal of Experimental Biology (2018) 221, jeb167742. doi:10.1242/jeb.167742

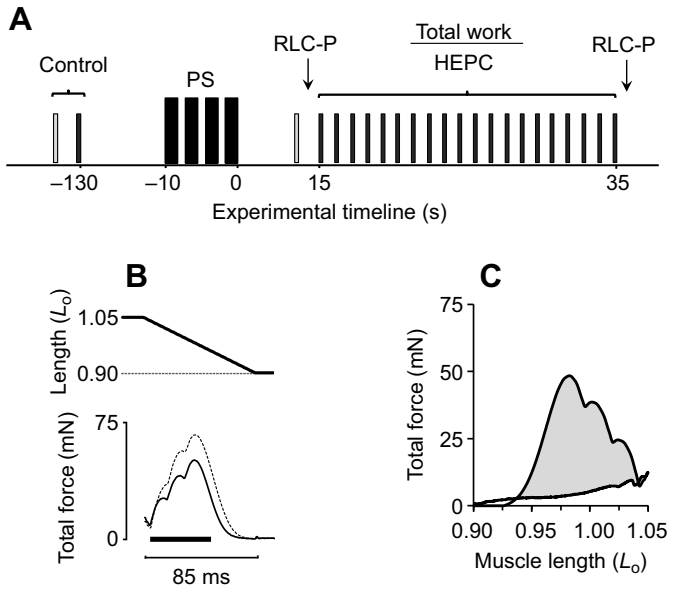

Fig. 1. Experimental timeline and details of the isovelocity shortening ramps used to calculate muscular work. (A) Experimental timeline utilized for all contractile experiments. Initially, a baseline force response (control) was elicited in the unpotentiated state; then, following the potentiating stimulus (PS), the identical parameters were repeated once per second for 20 s. For control and potentiated responses, a passive length ramp (open bars) without accompanying stimulation preceded active length ramps with stimulation (shaded bars). Prior to and following the series of potentiated stimuli, separate sets of muscles were frozen for biochemical analysis of myosin regulatory light chain (RLC) phosphorylation (RLC-P) and high-energy phosphate consumption (HEPC). (B) Example length and force traces during ramp shortening from 1.05 to 0.90 optimal length (L_o) at 0.40 maximal shortening velocity (V_{max}) for control (solid line) and potentiated (dashed line) responses. The thick black line represents the evoked stimulation period (50 ms, 75 Hz). (C) Example force–displacement plot ('work loop') that was used to quantify the work performed during each stimulus period.

Analysis of contractile parameters

The raw (total) and passive force traces for each stimulus were used to calculate the active force response of the muscle. Active forces were obtained by subtracting the passive force response from the matching total force response as previously described (Gittings et al., 2012). Peak force (mN) was calculated as the highest active force value reached during the stimulus period regardless of timing. Mechanical work (J kg^{-1}) was determined by calculating the integral of the force–displacement plot for each stimulus period and normalizing it to muscle wet mass. The kinetics of force development ($+dP/dt$) and relaxation ($-dP/dt$) were sampled at the start and end of each stimulation period from the first derivative function of the active force trace, expressed in mN s^{-1} [as described previously in Bowslaugh et al. (2016) and Gittings et al. (2012)].

HEPC

Separate sets of muscles from each genotype were rapidly frozen with liquid nitrogen-cooled tongs before and after the period of repeated concentric stimulation to assess the energetic cost associated with the work performed. Fluorometric assays were conducted on lyophilized (FreeZone 4.5, Labconco, Kansas City, MO, USA) and powdered whole-muscle homogenate samples following the removal of sutures and connective tissue. Powdered muscle samples were mixed thoroughly and aliquoted into 0.5 ml microcentrifuge tubes. Metabolites were extracted from aliquots of lyophilized tissue using 0.5 mol l^{-1} perchloric acid ($HClO_4$), and neutralized with 2.3 mol l^{-1} potassium carbonate ($KHCO_3$). The concentrations of metabolites were analyzed in triplicate using fluorometric techniques as previously described (Bergmeyer et al., 1983; Harris et al., 1974). Three assays were used to identify the relative concentration of the metabolites of interest, including ATP, phosphocreatine (PCr), creatine (Cr) and lactate. To adjust for variability in solid non-muscle constituents, all raw metabolite values were normalized to total Cr content (i.e. divided by the sum of PCr+Cr, then multiplied by mean total Cr content for the whole material) (Zhang et al., 2006). HEPC, a measure of ATP turnover determined through anaerobic ATP production, was determined from changes in PCr, lactate and ATP using the HEPC equation: $HEPC=1.5\Delta lactate-\Delta PCr-2\Delta[ATP]$. As the study design did not allow metabolite concentrations to be sampled from the same muscle at more than one time point, the delta term (Δ) signifies the differences in metabolite concentrations between distinct EDL muscles frozen before and after repetitive stimulation (i.e. post-PS versus final).

RLC phosphate content

Parallel experiments were conducted to determine RLC phosphorylation of WT and skMLCK$^{-/-}$ muscles sampled prior to and following the period of concentric work to coincide with the time points for HEPC analysis. Muscles were frozen with liquid nitrogen-cooled tongs and stored at −80°C until needed. RLC phosphorylation analysis was conducted using urea–glycerol PAGE as previously described (Gittings et al., 2016; Bowslaugh et al., 2016; Xeni et al., 2011), in accordance with the method conceived and subsequently described by Dr Jim Stull and co-workers (Manning and Stull, 1982; Zhi et al., 2005). The primary myosin RLC antibody used in the current work was originally purified by Dr Jim Stull (Department of Physiology, University of Texas Southwestern Medical Center) and was provided as a gift.

Statistical analysis

Two-tailed Student's *t*-tests were used to examine the effect of genotype (WT or skMLCK$^{-/-}$) on total work performed, changes in muscle metabolite concentrations, HEPC and economy. Following confirmation of homogeneity of variance, a two-way repeated measures ANOVA was conducted to test the effect of genotype (WT or skMLCK$^{-/-}$) on work per contraction during the period of repetitive stimulation (control versus post-PS versus final). To further evaluate significant interactions and planned comparisons (i.e. between genotypes), *post hoc* testing was performed using the Šidák correction. For all tests, the critical *P*-value for significance was $P<0.05$. All data are reported as means±s.e.m. Sample sizes (n) used in the current study to achieve adequate statistical power were based on previous results from our lab and others for mechanical (Gittings et al., 2011, 2012, 2016; Abbate et al., 2001) and biochemical (Zhi et al., 2005; Zhang et al., 2006) measurements and analysis.

RESULTS

EDL muscle characteristics

A summary of the mass, length and physiological cross-sectional area (PCSA) of EDL muscles utilized for contractile experiments is presented in Table 1. No genotype differences were evident for these measurements.

Table 2 contains isometric data for maximal twitch (P_t) and tetanic forces (P_o), as well as twitch:tetanus ratio, for WT and skMLCK$^{-/-}$ muscles. Maximal isometric twitch force was measured prior to any stimulation (i.e. unpotentiated), and peak tetanic force for each

Journal of Experimental Biology (2018) 221, jeb167742. doi:10.1242/jeb.167742

Table 1. Muscle characteristics from WT and skMLCK$^{-/-}$ mice

	Mass (mg)	Length (mm)	PCSA (mm^2)
WT	12.5±0.1	12.5±0.1	2.2±0.1
skMLCK$^{-/-}$	12.4±0.2	12.5±0.1	2.1±0.1

Data are from wild-type (WT) mice and those lacking skeletal myosin light chain kinase (skMLCK$^{-/-}$), and are presented as means±s.e.m. (n=8). PCSA, physiological cross-sectional area.

muscle was sampled from the first tetanus during the PS (note: stimulation occurred at 0.90 L_o because of the preceding control isovelocity stimulation). The forces produced during these high-frequency (100 Hz) volleys produces ≥95% of peak isometric tetanic force (P_o) that results from supramaximal stimulation normally elicited at 150–200 Hz. Therefore, to avoid additional supramaximal stimulation, the existing data from the first tetanus of the PS were used as a surrogate for P_o. No genotype differences in these measurements were found; moreover, the comparison of specific tension (force/PCSA) in WT and skMLCK$^{-/-}$ muscles did not reveal differences for twitches (31.7±2.3 and 31.0±2.5 mN mm^{-2}, respectively) or tetani (107.1±8.6 and 107.7±9.0 mN mm^{-2}, respectively).

Potentiation of concentric force and work during repetitive stimulation

An identical stimulation and ramp-shortening paradigm was elicited once before (control) and 20 times following the PS. Representative force traces are displayed in Fig. 2 for the control stimulation as well as the first and last stimuli in the potentiated train. Absolute force and work responses are presented in Table 3 and relative changes in work performed per stimulation (i.e. post-tetanic potentiation) are summarized in Fig. 3. Genotype differences in concentric force and work were evident in every comparison, including both control and potentiated responses (P<0.05). Following the PS, concentric forces were potentiated in both genotypes, although the effect was greater in WT than in skMLCK$^{-/-}$ muscles (to 1.38±0.03 and 1.10±0.04, respectively; P<0.05). During the 20 s of repetitive stimulation following the PS, skMLCK$^{-/-}$ forces were consistently potentiated between 9% and 15% above the control value. The magnitude of force potentiation in WT muscles during this period remained between 30% and 35%; however, the force response at stimulation no. 20 (final) was slightly lower than that at stimulation no. 1 (post-PS) (from 38% to 30%, respectively).

Analysis of the concentric portion of the force–displacement function for each stimulus (i.e. concentric work) showed that work increased significantly following the PS in both genotypes (to 1.10±0.05 and 1.51±0.03 in skMLCK$^{-/-}$ and WT muscles, respectively; P<0.05). As with peak force, the magnitude of the effect was significantly greater in WT than in skMLCK$^{-/-}$ muscles (P<0.05). Interestingly, although the potentiation effect in skMLCK$^{-/-}$ muscles for peak force and work was similar (10%), the enhancement of work in WT muscles was greater than the enhancement of peak force (51% versus 38%). The work performed during each of the 20 potentiated stimuli was summed for each muscle to quantify the total work performed in the potentiated state (see Fig. 4A). The moderate genotype difference in work per stimulation produced a substantial cumulative effect when pooled, as WT muscles performed ∼58% more total work than skMLCK$^{-/-}$ muscles in response to the same stimulus regime (P<0.05).

Table 2. Baseline isometric contractile parameters in WT and skMLCK$^{-/-}$ muscles

	P_t (mN)	P_o (mN)	P_t:P_o
WT	67.63±3.63	229.04±15.67	0.30±0.01
skMLCK$^{-/-}$	65.55±3.98	227.80±14.81	0.29±0.01

All data are presented as means±s.e.m. (n=8). P_t, peak twitch force; P_o, peak tetanic force (100 Hz); P_t:P_o, twitch to tetanus ratio.

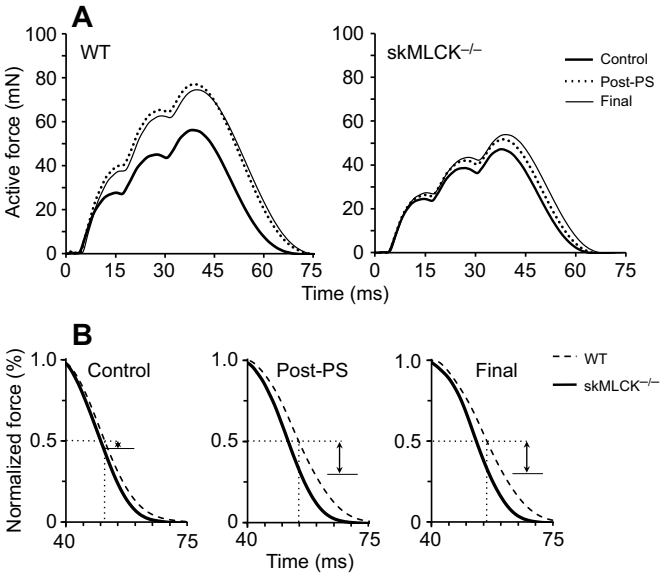

Fig. 2. Representative force traces during repetitive stimulation. (A) Representative active force traces in muscles from wild-type (WT) mice and those lacking skeletal myosin light chain kinase (skMLCK$^{-/-}$) before the PS (control) are superimposed with traces from the first (post-PS) and last (final) experimental stimuli in the potentiated state. (B) Normalized active force traces for the control activation prior to the PS, as well as for the first (post-PS) and last (final) of the repeated concentric activations in the potentiated state. In each panel, the thick line represents the average skMLCK$^{-/-}$ response and the dashed line represents the average WT response for all muscles used in the contractile experiments (n=8). Traces were normalized to their own peak force to illustrate differences between genotypes and in the shape of unfused tetani when potentiated. At the point of half-relaxation in WT muscles (dotted line), the corresponding relative force level in skMLCK$^{-/-}$ muscles was 0.45 (control), 0.32 (post-PS) and 0.32 (final).

Table 3. Concentric contractile parameters before and after the potentiating stimulus (PS)

	Control	Post-PS	Final
Peak force (mN)			
WT	53.57±2.05^a	73.61±2.23^c	69.09±1.9^b
skMLCK$^{-/-}$	43.17±1.85^{a,*}	47.54±2.98^{b,*}	48.07±3.00^{b,*}
Work per stimulus (J kg^{-1})			
WT	3.21±0.17^a	4.81±0.19^c	4.59±0.18^b
skMLCK$^{-/-}$	2.55±0.15^{a,*}	2.82±0.18^{b,*}	2.97±0.23^{b,*}
+dP/dt (mN s^{-1})			
WT	2303±89^a	2992±132^c	2718±134^b
skMLCK$^{-/-}$	2143±81^a	2407±129^{b,*}	2467±138^b
−dP/dt (mN s^{-1})			
WT	1659±51^a	1901±75^b	1727±90^a
skMLCK$^{-/-}$	1411±67^{a,*}	1601±86^{b,*}	1538±64^{b,*}

All data are presented as means±s.e.m. (n=8). +dP/dt, rate of force development; −dP/dt, rate of force relaxation. Two-way RM ANOVA, Šidák correction for multiple comparisons.
*skMLCK$^{-/-}$ value is less than WT value (P<0.05).
^{a,b,c} Within-genotype comparisons between control, post-PS and final (P<0.05).

Journal of Experimental Biology (2018) 221, jeb167742. doi:10.1242/jeb.167742

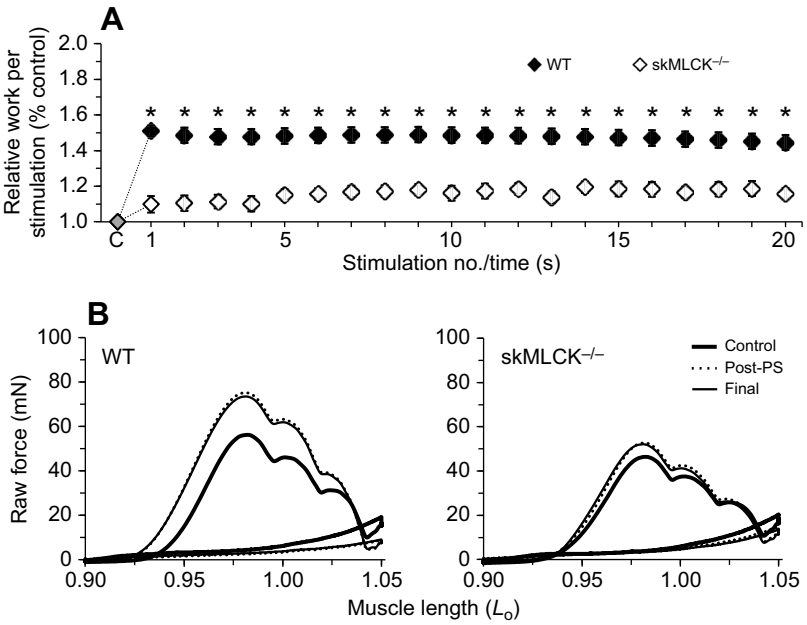

Fig. 3. Post-tetanic potentiation. (A) Relative change in work performed per stimulation (i.e. potentiation) when compared with the control response for each genotype. *WT value is greater than the corresponding skMLCK$^{-/-}$ value at each time point (means±s.e.m., RM ANOVA Šidák correction for multiple comparisons, P<0.05, n=8). (B) Representative work loop traces from WT and skMLCK$^{-/-}$ muscles prior to the PS (control) as well as during the first (post-PS) and last (final) of the potentiated state.

Kinetics of force development and relaxation

Summary data for rate of force development (+dP/dt) and rate of relaxation (−dP/dt) during the control condition, as well as during the first (post-PS) and last (final) of the potentiated stimuli are presented in Table 3. Although there were no genotype differences in +dP/dt during the control condition, the WT value was greater than the skMLCK$^{-/-}$ value following the PS (P<0.05). This represents a relative increase of ∼30% in WT muscles versus ∼12% in skMLCK$^{-/-}$ muscles as a result of the PS. This genotype difference was not maintained until the end of the stimulation period, although WT and skMLCK$^{-/-}$ values were both still elevated above the control value (1.18±0.03 and 1.15±0.02, respectively; P<0.05). Interestingly, the rate of force relaxation (−dP/dt) was faster in WT muscles than in skMLCK$^{-/-}$ muscles before and following the PS (P<0.05). Following the PS, −dP/dt increased similarly in the two genotypes (∼15%; P<0.05). The faster kinetics of relaxation persisted throughout the potentiated stimulation period in skMLCK$^{-/-}$ muscles but WT values returned to near-control values by the end of the stimulation period (final).

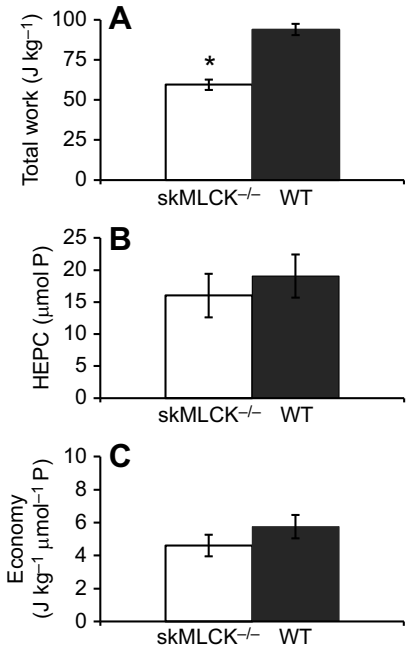

Fig. 4. Total work, HEPC and economy during repeated stimulation. (A) Total work performed during the series of repeated stimuli that followed the potentiating stimulus. *skMLCK$^{-/-}$ muscles performed significantly less total work than WT muscles (means±s.e.m., two-tailed Student's t-test, P<0.05, n=8). (B) HEPC calculated from muscle metabolite values measured in frozen muscle homogenates (means±s.e.m., two-tailed Student's t-test, P<0.05, n=8). (C) Economy (i.e. total work/HEPC) during repeated stimulation in WT and skMLCK$^{-/-}$ muscles (means±s.e.m., two-tailed Student's t-test, P<0.05, n=8).

Muscle metabolites

Fluorometric assays were used to determine the concentration of ATP, PCr, Cr and lactate in samples extracted from muscles frozen before and after the period of repetitive concentric stimulation (n=8). In both genotypes, this activation resulted in a depletion of [PCr] and an accumulation of [Cr] and [lactate] (P<0.05). In contrast, [ATP] levels were sustained in both genotypes when samples frozen before and after stimulation were compared. Within each genotype, the differences in muscle metabolite concentrations between time points (i.e. post-PS versus final) were used to estimate the energetic cost of the muscular work performed (i.e. anaerobic ATP turnover). Table 4 includes the mean difference terms for each genotype (i.e. −2Δ[ATP], Δ[PCr], 1.5Δ[lactate]). Of these values, only lactate values were different between genotypes, as the increase in [lactate] following the stimulation period was smaller in skMLCK$^{-/-}$ versus WT muscles (P<0.05). In both genotypes, the

Table 4. High-energy phosphate consumption: difference terms for HEPC calculation

	−2Δ[ATP]	Δ[PCr]	1.5Δ[Lactate]
WT	−0.47±1.41	10.80±2.79	7.45±0.22
skMLCK$^{-/-}$	0.89±0.91	10.11±3.43	4.88±0.42*

All data are presented as means±s.e.m. (n=8).
*skMLCK$^{-/-}$ value is significantly lower than WT value (two-way Student's t-test, P<0.05).

Journal of Experimental Biology (2018) 221, jeb167742. doi:10.1242/jeb.167742

degradation of PCr was similar and, as mentioned above, ATP levels were not significantly different when compared before and after the experimental stimulation regime (i.e. ATP levels were buffered). The results of HEPC calculations are shown in Fig. 4B for all WT and skMLCK$^{-/-}$ muscles. Although WT values for HEPC were ∼18% greater than those for skMLCK$^{-/-}$, this difference was not statistically significant (P=0.27) (Table S1).

Economy

The contractile economy for each genotype was calculated from the total work performed by each muscle and the HEPC calculated between paired muscles frozen before and after the period of stimulation. Fig. 4C presents the results of this analysis for WT and skMLCK$^{-/-}$ muscles. Importantly, there was no statistical difference in economy between the genotypes (P=0.27). This result was produced by opposing outcomes observed in contractile versus biochemical analyses; specifically, the robust enhancement of work performed in WT muscles was associated with a small (∼18%) but non-significant increase in HEPC.

RLC phosphorylation

Representative blots and summary data for RLC phosphorylation of WT and skMLCK$^{-/-}$ muscles are shown in Fig. 5. As expected, WT samples frozen after the PS and following stimulation displayed a prominent phosphorylated band that was similar between these time points spanning the interval over which total work and HEPC were measured. In contrast, skMLCK$^{-/-}$ samples frozen following the PS or the 20 s period of intermittent stimulation did not display an obvious or consistent phosphorylated band. Consistent with previous reports, a low level of baseline RLC phosphorylation was present (∼2–3%) although clear phosphorylated RLC bands were not consistently present in skMLCK$^{-/-}$ muscles. This may result from the phosphorylation of an adjacent serine residue by an undetermined kinase that is stimulation independent (Zhi et al., 2005).

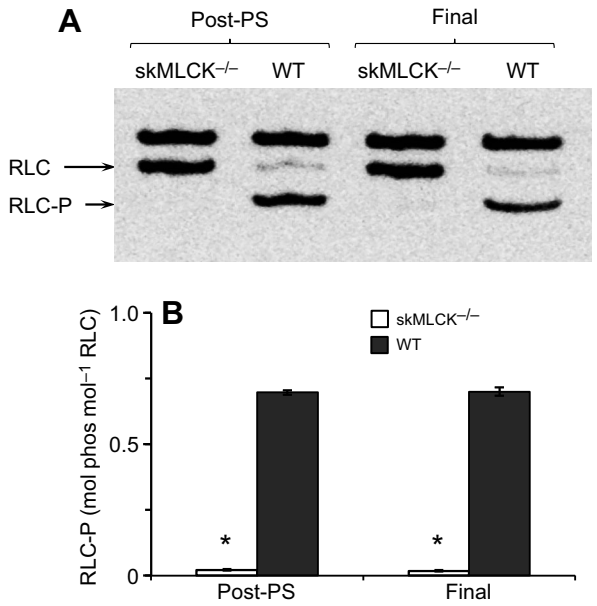

Fig. 5. RLC phosphorylation. (A) Representative blots from urea–glycerol PAGE analysis of WT and skMLCK$^{-/-}$ whole-muscle homogenates quick-frozen before and immediately after the period of repeated stimulation. Protein density was measured using Image Studio Lite (LI-COR Biosciences, Lincoln, NE, USA), and fractional RLC phosphate content was calculated as the ratio of the phosphorylated band to total light chain content (RLC phosphorylation=[RLC-P]/[RLC]+[RLC-P]). (B) Myosin RLC phosphate content in WT and skMLCK$^{-/-}$ muscles. *skMLCK$^{-/-}$ value is less than the corresponding WT value (means±s.e.m., two-way ANOVA, P<0.05, n=4).

DISCUSSION

The purpose of this study was to compare the contractile economy of repeated isotonic contractions in potentiated mouse fast muscle with and without the ability to phosphorylate the myosin RLC. Our main finding was that WT muscles performed more work per contraction and thus performed more total work than skMLCK$^{-/-}$ muscles without a proportional increase in energy turnover. These results suggest that skMLCK-catalyzed phosphorylation of the RLC does not greatly increase the energetic 'overhead' of repeated dynamic contractions close to peak power. Thus, although we hypothesized that WT muscles would display a decreased economy compared with skMLCK$^{-/-}$ muscles, we must reject this and accept the null hypothesis that RLC phosphorylation-mediated potentiation does not decrease the economy of mouse EDL muscle.

Implications of RLC phosphorylation-mediated potentiation on energetics and economy

The skMLCK-catalyzed phosphorylation of the RLC is associated with potentiation of concentric force, work and power in mouse (Gittings et al., 2011, 2012, 2015, 2016; Zhi et al., 2005; Bowslaugh et al., 2016; Caterini et al., 2011; Grange et al., 1995, 1998), cat (Brown and Loeb, 1998, 1999) and rat (Macintosh and Bryan, 2002; Macintosh et al., 2008b; Macintosh and Willis, 2000) skeletal muscle models. The effect of RLC phosphorylation-mediated force potentiation on muscle energetics is poorly understood, however. Studies attempting to elucidate the relative contribution of the major ATP using processes in skeletal muscle (i.e. Na^+/K^+-ATPase, SERCA, myosin-ATPase) do not account for the ATP cost of RLC phosphorylation (Zhang et al., 2006; Barclay et al., 2008). Although unmeasured, it has been argued that the energy cost for the skMLCK-catalyzed phosphorylation of RLC may be only ∼5% of muscle ATPase during contraction (Homsher, 1987). Although we could not quantify the energetic cost of increased work performed from any energy cost for RLC phosphorylation, our results showing no statistical difference in HEPC turnover between WT and skMLCK$^{-/-}$ muscles support the idea that the energetic overhead of skMLCK activity is minor when measured against the background of the overall muscle ATPase activity. Indeed, a prediction of work performed on permeabilized rabbit psoas skeletal fibers during steady-state contractions is that RLC phosphorylation should increase myosin ATPase rate in proportion to force levels (Sweeney and Stull, 1990). If these results can be extrapolated to the current concentric contractions in intact muscles, they predict that a disproportionate increase to HEPC during potentiation could be assigned to: (i) the ATP cost of skMLCK phosphotransferase activity, (ii) an increase in the ATP cost of ion trafficking by Na^+/K^+ or SERCA pumps, or (iii) the increased work performed as a result of myosin RLC phosphorylation. At present, without a significant difference in HEPC observed between genotypes, and without prior report that myosin RLC phosphorylation directly modulates the mechanisms of ion trafficking, we must consider the relationship between increased work and potentiation. To this end, a possible explanation for why WT muscles were able to perform more work without an attendant increase in HEPC compared with skMLCK$^{-/-}$ muscles comes from Greenberg et al. (2009, 2010), who used contractile proteins isolated from rabbit psoas muscle in an *in vitro* motility assay. Their data suggest that RLC phosphorylation alters

the strain-dependent release of ADP following the power stroke, an effect that may prolong the duty cycle, and thus the work performed, by the attached cross-bridge during each ATPase cycle (Greenburg et al., 2009, 2010). Interestingly, this effect of RLC phosphorylation may not be present at very low loads, explaining why this molecular mechanism does not appear to alter unloaded shortening velocity of permeabilized fibers (Persechini et al., 1985) or intact muscle (Gittings et al., 2011; Palmer and Moore, 1989) (cf. Grange et al., 1995). Taken together, these observations may account for why work can increase without a proportional increase in HEPC in WT muscles.

Another aspect of our data that may help account for our observation of increased work without a commensurate increase in HEPC was the prolongation of relaxation from tetanic force observed in WT but not skMLCK$^{-/-}$ muscles. Similar observations of slowed relaxation have been made in intact mouse and cat muscle (Gittings et al., 2011; Brown and Loeb, 1999). Analogous effects have been observed in permeabilized rabbit psoas fibers (Patel et al., 1998) and attributed to an ability of RLC phosphorylation to slow the rate constant for transition of cross-bridges from strongly bound to weakly bound states or to a disruption of Ca^{2+} and cross-bridge activation-dependent changes in relaxation rates. Taken together, these studies suggest that the genotype difference in relative force level at the same time point shown in Fig. 2 may underlie the significant difference in work performed per contraction between WT and skMLCK$^{-/-}$ muscles. Importantly, these changes are evident despite no genotype differences in force relaxation rates ($-dP/dt$).

Comparison with relevant literature

Our results are not in agreement with experiments showing that the economy of rat hindlimb muscles *in situ* was reduced by potentiation (Abbate et al., 2001). These investigators measured total work and HEPC in two groups during 10 repetitive concentric contractions at 60 Hz; in one group, the series of contractions was preceded by an isometric potentiating stimulus (PRC) that served to pre-elevate RLC phosphorylation and the other was not (RC). Although the total work performed in the PRC condition was 20% higher than that in the RC condition, HEPC was increased by 40% in the PRC versus RC condition, thus lowering overall economy. The increase in HEPC was attributed to the increased ATPase of the contractile apparatus, and not to RLC phosphorylation itself as this was similar (~40%) at the conclusion of the RC and the PRC groups. Interestingly, inspection of their force traces revealed a gradual increase in force (i.e. staircase potentiation), suggesting a gradual increase in RLC phosphorylation in the RC group. Finally, the PRC group received significantly more total stimulation than the RC group (1 s of 160 Hz stimulation), a fact that perhaps contributed to the disproportionate increase in HEPC in this condition. As a result, these experiments may not represent the true difference in energetics, work or economy between the unphosphorylated and phosphorylated states. Advantages of the present study include the fact that our use of skMLCK$^{-/-}$ muscles allowed us to establish a true 'control' condition without RLC phosphorylation-mediated potentiation. In addition, the two groups received identical stimulation and performed a steady-state level of work per contraction in both conditions; thus, our comparisons of HEPC and work between unphosphorylated and phosphorylated states are the most robust that have been reported to date.

Potentiation in skMLCK$^{-/-}$ muscles

The potentiation displayed by skMLCK$^{-/-}$ muscles in the current study is part of the mounting evidence for alternative mechanism(s) that may modulate contractile function independent of RLC phosphorylation in WT muscles (Zhi et al., 2005). For example, in mouse lumbrical muscles, isometric twitch potentiation in the absence of RLC phosphorylation has been associated with stimulation-induced elevations in resting myoplasmic Ca^{2+} levels (Smith et al., 2013). Although this effect was relatively small and dissipated rapidly (≤20 s at 37°C), this mechanism may provide an explanation for the potentiation observed in the present study as well as by others (Macintosh et al., 2008a; Rassier et al., 1999) in the absence of RLC phosphorylation. In the current experiments, the stimulation protocol did not commence until ~15 s after the PS, perhaps minimizing the ability of this mechanism to contribute. In support of this idea are our data showing a stable level of potentiation between 15 and 35 s in skMLCK$^{-/-}$ muscles. By extension, it also seems possible that the low duty cycle (0.05 Hz) we used in our experiments may have maintained or prolonged any increase in resting myoplasmic Ca^{2+} levels for the duration of the time period investigated. The increase in force and work displayed by our skMLCK$^{-/-}$ muscles was small relative to the WT response (~10 versus 40–50%, respectively). If we make the assumption that this RLC phosphorylation-independent mechanism of force enhancement was present in WT muscles, it may produce 20–25% of the potentiation displayed by this genotype. Interestingly, this RLC phosphorylation-independent potentiation may be contraction-type dependent as skMLCK$^{-/-}$ muscles display post-tetanic depression of isometric forces under similar conditions (Gittings et al., 2015). Thus, our use of concentric (isovelocity) contractions may have optimized the influence of both RLC phosphorylation-dependent and -independent forms of potentiation.

Limitations

Our measurement of the energetic cost for work does not incorporate the aerobic contribution to total ATP usage; therefore, the measurement of HEPC represents the energy used for substrate-level metabolic processes only. Westra et al. (1988) have reported that for sustained isometric tetani at 60 Hz up to 30 s, aerobic contribution to total energy turnover is ≤9% (rat quadriceps, 35°C). Because the muscle used in that study had a more oxidative profile than mouse EDL (Ariano et al., 1973; Delp and Duan, 1996), this estimate of aerobic contribution may even be an overestimation. Moreover, in addition to species and fiber type, muscle energetics is sensitive to a variety of experimental factors including stimulation frequency and duration, duty cycle, contraction type, muscle length and temperature (Rall, 1984). The utilization of different stimulus and/or shortening ramp parameters may have revealed differences our experimental design did not, as would improved methods of measurement of HEPC. Finally, although our measurements could not ascertain the HEPC associated with RLC phosphorylation-independent potentiation in either genotype, our direct comparisons of WT and skMLCK$^{-/-}$ muscles subjected to identical stimulation warrant a view that RLC phosphorylation-dependent potentiation is metabolically sustainable.

Conclusions

We found that WT muscles with RLC phosphorylation performed significantly more work per contraction than skMLCK$^{-/-}$ muscles that operated in the absence of RLC phosphorylation. These results are part of the mounting evidence that skMLCK-catalyzed phosphorylation of the RLC modulates both submaximal and maximal dynamic function of the mammalian fast-twitch muscle phenotype. Further, although other mechanisms for potentiation clearly exist, this study suggests that the energetic overhead for

skMLCK-catalyzed phosphorylation of the RLC is not sufficient to decrease the economy of mouse EDL muscle at 25°C.

Our findings support the depiction of myosin RLC phosphorylation as an ideal modulatory mechanism in skeletal muscle because of its low energy requirement (Sweeney et al., 1993), where the metabolic cost of this mechanism is minimized by the restriction of skMLCK to operation primarily during muscle activity (Ca^{2+} dependency) and the relatively high ratio of kinase to phosphatase activity that is characteristic of fast isoforms (Stull et al., 2011). Therefore, the capacity to maximize force and/or work output while remaining metabolically sustainable is likely to be the most physiologically significant aspect of RLC phosphorylation, especially given the propensity of fast skeletal muscles to fatigue. However, there is other evidence that RLC phosphorylation may be physiologically significant beyond the simple enhancement of mechanical function, including the capacity to maintain submaximal force output at lower levels of motor drive/motor unit firing in the potentiated state (Klein et al., 2001; Inglis et al., 2011), involvement in the regulation of the so-called super-relaxed state of myosin that is implicated in adaptive thermogenesis (Cooke, 2011), and modulation of muscle contractility in female mice through estradiol's effect on RLC phosphorylation (Lai et al., 2016). Thus, it is increasingly apparent that beyond the well-studied mechanical outcomes associated with myosin RLC phosphorylation, this mechanism may act at the intersection point of a variety of physiological systems that both acutely and chronically modulate skeletal muscle function.

Acknowledgements
The authors would like to acknowledge the support of Dr J Stull (Department of Physiology, University of Texas Southwestern Medical Center) in development of the skMLCK$^{-/-}$ mouse colony and with methods for quantification of myosin RLC phosphate content.

Competing interests
The authors declare no competing or financial interests.

Author contributions
Conceptualization: W.G., J.B., R.V.; Methodology: W.G., J.B., R.V.; Formal analysis: W.G.; Investigation: W.G.; Resources: R.V.; Writing - original draft: W.G.; Writing - review & editing: W.G., J.B., R.V.; Supervision: R.V.; Project administration: R.V.; Funding acquisition: R.V.

Funding
This research was made possible by funding from the Natural Sciences and Engineering Council of Canada (RV Discovery Grant: 2014-05122).

Data availability
The datasets used and/or analyzed during the current study are available from the corresponding author on request.

Supplementary information
Supplementary information available online at
http://jeb.biologists.org/lookup/doi/10.1242/jeb.167742.supplemental

References
Abbate, F., Van Der Velden, J., Stienen, G. J. and de Haan, A. (2001). Post-tetanic potentiation increases energy cost to a higher extent than work in rat fast skeletal muscle. *J. Musc. Res. Cell Motil.* **22**, 703-710.
Ariano, M. A., Edgerton, V. R. and Armstrong, R. B. (1973). Hindlimb muscle fiber populations of five mammals. *J. Histo. Cyto.* **21**, 51-55.
Barclay, C. J., Lichtwark, G. A. and Curtin, N. A. (2008). The energetic cost of activation in mouse fast-twitch muscle is the same whether measured using reduced filament overlap or N-benzyl-p-toluenesulphonamide. *Acta Physiologica* **193**, 381-391.
Barsotti, R. J. and Butler, T. M. (1984). Chemical energy usage and myosin light chain phosphorylation in mammalian skeletal muscle. *J. Musc. Res. Cell Motil.* **5**, 45-64.
Bergmeyer, H. U., Grabl, M. and Walter, H. E. (1983). *Methods of Enzymatic Analysis*. Weinhein: Verlag-Chemie.
Bowslaugh, J., Gittings, W. and Vandenboom, R. (2016). Myosin light chain phosphorylation is required for peak power output of mouse fast skeletal muscle in vitro. *Pflugers Archive-Eur. J. Physiol.* **468**, 2007-2016.
Brown, I. E. and Loeb, G. E. (1998). Post-activation potentiation: a clue for simplifying models of muscle dynamics. *Am. Zool.* **38**(4), 743-754.
Brown, I. E. and Loeb, G. E. (1999). Measured and modeled properties of mammalian skeletal muscle. I. The effects of post-activation potentiation on the time course and velocity dependencies of force production. *J. Musc. Res. Cell Motil.* **20**, 443-456.
Butler, T. M., Siegman, M. J., Mooers, S. U. and Barsotti, R. J. (1983). Myosin light chain phosphorylation does not modulate cross-bridge cycling rate in mouse skeletal muscle. *Science* **220**, 1167-1169.
Caterini, D., Gittings, W., Huang, J. and Vandenboom, R. (2011). The effect of work cycle frequency on the potentiation of dynamic force in mouse fast twitch skeletal muscle. *J. Exp. Biol.* **214**, 3915-3923.
Cooke, R. (2011). The role of the myosin ATPase activity in adaptive thermogenesis by skeletal muscle. *Biophys. Rev.* **3**, 33.
Crow, M. T. and Kushmerick, M. J. (1982a). Myosin light chain phosphorylation is associated with a decrease in the energy cost for contraction in fast twitch mouse muscle. *J. Biol. Chem.* **257**, 2121-2124.
Crow, M. T. and Kushmerick, M. J. (1982b). Phosphorylation of myosin light chains in mouse fast-twitch muscle associated with reduced actomyosin turnover rate. *Science* **217**, 835-837.
Delp, M. D. and Duan, C. (1996). Composition and size of type I, IIA, IID/X, and IIB fibers and citrate synthase activity of rat muscle. *J. Appl. Physiol.* **80**, 261-270.
Edman, K. A. (1979). The velocity of unloaded shortening and its relation to sarcomere length and isometric force in vertebrate muscle fibres. *J. Physiol.* **291**, 143.
Gittings, W., Huang, J., Smith, I. C., Quadrilatero, J. and Vandenboom, R. (2011). The effect of skeletal myosin light chain kinase gene ablation on the fatigability of mouse fast muscle. *J. Musc. Res. Cell Motil.* **31**, 337-348.
Gittings, W., Huang, J. and Vandenboom, R. (2012). Tetanic force potentiation of mouse fast muscle is shortening speed dependent. *J. Musc. Res. Cell Motil.* **33**, 359-368.
Gittings, W., Aggarwal, H., Stull, J. T. and Vandenboom, R. (2015). The force dependence of isometric and concentric potentiation in mouse muscle with and without skeletal myosin light chain kinase. *Can. J. Physiol. Pharmacol.* **93**, 23-32.
Gittings, W., Bunda, J., Stull, J. T. and Vandenboom, R. (2016). Interaction of posttetanic potentiation and the catchlike property in mouse skeletal muscle. *Muscle Nerve.* **54**, 308-316.
Godt, R. E. and Nosek, T. M. (1989). Changes of intracellular milieu with fatigue or hypoxia depress contraction of skinned rabbit skeletal and cardiac muscle. *J. Physiol.* **412**, 155-180.
Gordon, D. A., Enoka, R. M. and Stuart, D. G. (1990). Motor-unit force potentiation in adult cats during a standard fatigue test. *J. Physiol.* **421**, 569-582.
Grange, R. W., Cory, C. R., Vandenboom, R. and Houston, M. E. (1995). Myosin phosphorylation augments force-displacement and force-velocity relationships of mouse fast muscle. *Am. J. Physiol.* **269**, C713-C724.
Grange, R. W., Vandenboom, R., Xeni, J. and Houston, M. E. (1998). Potentiation of in vitro concentric work in mouse fast muscle. *J. Appl. Physiol.* **84**, 236-243.
Greenberg, M. J., Mealy, T. R., Watt, J. D., Jones, M., Szczesna-Cordary, D. and Moore, J. R. (2009). The molecular effects of skeletal muscle myosin regulatory light chain phosphorylation. *Am. J. Physiol.***297**, R265-R274.
Greenberg, M. J., Mealy, T. R., Jones, M., Szczesna-Cordary, D. and Moore, J. R. (2010). The direct molecular effects of fatigue and myosin regulatory light chain phosphorylation on the actomyosin contractile apparatus. *Am. J. Physiol.* **298**, 989-996.
Harris, R. C., Hultman, E. and Nordesjö, L. O. (1974). Glycogen, glycolytic intermediates and high-energy phosphates determined in biopsy samples of musculus quadriceps femoris of man at rest. Methods and variance of values. *Scan. J. Clin. Lab. Invest.* **33**, 109-120.
Homsher, E. (1987). Muscle enthalpy production and its relationship to actomyosin ATPase. *Ann. Rev. Physiol.* **49**, 673-690.
Inglis, J. G., Howard, J., McIntosh, K., Gabriel, D. A. and Vandenboom, R. (2011). Decreased motor unit discharge rate in the potentiated human tibialis anterior muscle. *Acta. Physiologica.* **201**, 483-492.
Klein, C. S., Ivanova, T. D., Rice, C. L. and Garland, S. J. (2001). Motor unit discharge rate following twitch potentiation in human triceps brachii muscle. *Neurosci. Lett.* **316**, 153-156.
Lai, S., Collins, B. C., Colson, B. A., Kararigas, G. and Lowe, D. A. (2016). Estradiol modulates myosin regulatory light chain phosphorylation and contractility in skeletal muscle of female mice. *Am. J. Physiol. Endocrinol. Metab.* **310**, E724-E733.
Länngergren, J., Bruton, J. D. and Westerblad, H. (2000). Vacuole formation in fatigued skeletal muscle fibres from frog and mouse: effects of extracellular lactate. *J. Physiol.* **526**, 597-611.
Macintosh, B. R. and Bryan, S. N. (2002). Potentiation of shortening and velocity of shortening during repeated isotonic tetanic contractions in mammalian skeletal muscle. *Pflügers Archiv.* **443**, 804-812.

MacIntosh, B. R. and Willis, J. C. (2000). Force-frequency relationship and potentiation in mammalian skeletal muscle. *J. Appl. Physiol.* **88**, 2088-2096.
MacIntosh, B. R., Smith, M. J. and Rassier, D. E. (2008a). Staircase but not posttetanic potentiation in rat muscle after spinal cord hemisection. *Muscle Nerve.* **38**, 1455-1465.
Macintosh, B. R., Taub, E. C., Dormer, G. N. and Tomaras, E. K. (2008b). Potentiation of isometric and isotonic contractions during high-frequency stimulation. *Pflügers Archiv.* **456**, 449-458.
Macintosh, B. R., Holash, R. J. and Renaud, J. M. (2012). Skeletal muscle fatigue–regulation of excitation-contraction coupling to avoid metabolic catastrophe. *J. Cell Sci.* **125**, 2105-2114.
Manning, D. R. and Stull, J. T. (1982). Myosin light chain phosphorylation-dephosphorylation in mammalian skeletal muscle. *Am. J. Physiol.* **242**, C234-C241.
Myburgh, K. M. (2004). Protecting muscle ATP: positive roles for peripheral defense mechanisms-introduction. *Med. Sci. Spor. Exerc.* **36**, 16-19.
Palmer, B. M. and Moore, R. L. (1989). Myosin light chain phosphorylation and tension potentiation in mouse skeletal muscle. *Am. J. Physiol.* **257**, C1012-C1019.
Patel, J. R., Diffee, G. M., Huang, X. P. and Moss, R. L. (1998). Phosphorylation of myosin regulatory light chain eliminates force-dependent changes in relaxation rates in skeletal muscle. *Biophys. J.* **74**, 360-368.
Persechini, A., Stull, J. T. and Cooke, R. (1985). The effect of myosin phosphorylation on the contractile properties of skinned rabbit skeletal muscle fibers. *J. Biol. Chem.* **260**, 7951-7954.
Rall, J. A. (1984). Energetic aspects of skeletal muscle contraction: implications of fiber types. *Exer. Sport Sci. Rev.* **13**, 33-74.
Rankin, L. L., Enoka, R. M., Volz, K. A. and Stuart, D. G. (1988). Coexistence of twitch potentiation and tetanic force decline in rat hindlimb muscle. *J. Appl. Physiol.* **65**, 2687-2695.
Rassier, D. E. and MacIntosh, B. R. (2000). Coexistence of potentiation and fatigue in skeletal muscle. *Braz. J. Med. Biol. Res.* **33**, 499-508.
Rassier, D. E., Tubman, L. A. and MacIntosh, B. R. (1999). Staircase in mammalian muscle without light chain phosphorylation. *Braz. J. Med. Biol. Res.* **32**, 121-129.
Smith, I. C., Gittings, W., Huang, J., McMillan, E. M., Quadrilatero, J., Tupling, A. R. and Vandenboom, R. (2013). Potentiation in mouse lumbrical muscle without myosin light chain phosphorylation: is resting calcium responsible? *J. Gen. Physiol.* **141**, 297-308.
Stull, J. T., Kamm, K. E. and Vandenboom, R. (2011). Myosin light chain kinase and the role of myosin light chain phosphorylation in skeletal muscle. *Arch. Biochem. Biophys.* **510**, 120-128.
Sweeney, H. L. and Stull, J. T. (1990). Alteration of cross-bridge kinetics by myosin light chain phosphorylation in rabbit skeletal muscle: implications for regulation of actin-myosin interaction. *Proc. Natl. Acad. Sci. USA* **87**, 414-418.
Sweeney, H. L., Bowman, B. F. and Stull, J. T. (1993). Myosin light chain phosphorylation in vertebrate striated muscle: regulation and function. *Am. J. Physiol. Cell Physiol.* **264**, C1085-C1095.
Vandenboom, R. and Houston, M. E. (1996). Phosphorylation of myosin and twitch potentiation in fatigued skeletal muscle. *Can. J. Physiol. Pharmacol.* **74**, 1315-1321.
Vandenboom, R., Gittings, W., Smith, I. C., Grange, R. W. and Stull, J. T. (2013). Myosin phosphorylation and force potentiation in skeletal muscle: evidence from animal models. *J. Musc. Res. Cell Motil.* **34**, 317-332.
Westerblad, H., Bruton, J. D. and Katz, A. (2010). Skeletal muscle: Energy metabolism, fiber types, fatigue and adaptability. *Exp. Cell Res.* **316**, 3093-3099.
Westra, H. G., de Haan, A., van Doorn, J. E. and de Haan, E. J. (1988). Anaerobic chemical changes and mechanical output during isometric tetani of rat skeletal muscle in situ. *Pflüeg Archiv.* **412**, 121-127.
Xeni, J., Gittings, W., Caterini, D., Huang, J., Houston, M. E., Grange, R. W. and Vandenboom, R. (2011). Myosin light chain phosphorylation and potentiation of dynamic function in mouse fast muscle. *Pflugers Arch.* **362**, 349-358.
Zhang, S.-J., Andersson, D. C., Sandström, M. E., Westerblad, H. and Katz, A. (2006). Cross bridges account for only 20% of total ATP consumption during submaximal isometric contraction in mouse fast-twitch skeletal muscle. *Am. J. Physiol. Cell Physiol.* **291**, C147-C154.
Zhi, G., Ryder, J. W., Huang, J., Ding, P., Chen, Y., Zhao, Y., Kamm, K. E. and Stull, J. T. (2005). Myosin light chain kinase and myosin phosphorylation effect frequency-dependent potentiation of skeletal muscle contraction. *Proc. Nat. Acad. Sci. USA* **102**, 17519-17524.